Mathematical Finance
Picture Book

Christian Fries

Mathematical Finance Picture Book

Christian P. Fries

July 26, 2007

Version 0.4.0. Build 20070725.

Typeset by the author using TeXShop for Mac OS X™. Drawings by the author using OmniGraffle for Mac OS X™. Charts created using Java™ code by the author.

Version 0.4.0. Build 20070725.- July 26, 2007
http://www.christian-fries.de/finmath/mafipi

Preface

This picture book is a companion to *Mathematical Finance: Theory, Modeling, Implementation*. ISBN 0-470-04722-4.

Licence

Suggested citation

FRIES, CHRISTIAN P.: Mathematical Finance: Picture Book. Frankfurt am Main, 2007. http://www.christian-fries.de/finmath/mafipi.

Version 0.4.0. Build 20070725.- July 26, 2007
http://www.christian-fries.de/finmath/mafipi

Contents

1 Introduction

This books present some aspects in the realm of mathematical finance, specifically mathematical modeling for derivative pricing. The aspects are presented by pictures with brief annotations. For an in depth discussion of the underlying theory see *Fries, Christian: Mathematical Finance: Theory, Modeling, Implementation* (ISBN 0-470-04722-4).

1.1 Figure Number Mapping

The following tables give the mapping from the figure numbers of *Mathematical Finance* (left) to the figure number in this book (right).

B.1	→	2.1	21.2	→	4.2	18.7	→	5.6
B.2	→	2.2	21.3	→	4.3	18.8	→	5.7
B.3	→	2.3	21.4	→	4.4	18.9	→	5.8
25.1	→	3.1	18.2	→	5.1	18.10	→	5.9
25.2	→	3.2	18.3	→	5.2	18.11	→	5.10
25.3	→	3.3	18.4	→	5.3			
25.4	→	3.4	18.5	→	5.4			
21.1	→	4.1	18.6	→	5.5			

2 Factor Reduction

Let $R = (\rho_{i,j})_{i,j=1\ldots n}$ denote a given correlation matrix. Thus R is symmetric and positive semidefinite. This implies that R has real eigenvalues $\lambda_1 \geq \cdots \geq \lambda_n \geq 0$ and that a corresponding orthonormal basis of eigenvectors $v_1, \ldots, v_n$ of R exists, i.e.,

$$\exists\, V: \quad V^\top R V = D := \begin{pmatrix} \lambda_1 & & 0 \\ 0 & \ddots & 0 \\ 0 & & \lambda_n \end{pmatrix}, \qquad \text{where } V = (v_1, \ldots, v_n),$$

and $R = VDV^\top$ as well as $V^\top V = I$. Let $U_1, \ldots, U_n$ denote independent Brownian motions, $U := (U_1, \ldots, U_n)^\top$. Then W with

$$\mathrm{d}W := (\mathrm{d}W_1, \ldots, \mathrm{d}W_n)^\top := V \sqrt{D}\, \mathrm{d}U$$

is an n-dimensional Brownian motion with

$$< \mathrm{d}W_i, \mathrm{d}W_j >= \rho_{i,j}\, \mathrm{d}t.$$

With $F := (v_1 \sqrt{\lambda_1}, \ldots, v_n \sqrt{\lambda_n})$ we thus have $\mathrm{d}W = F\, \mathrm{d}U$. Let $m < n$. Using

$$(f_1, \ldots, f_n) \;=\; F \;=\; V\sqrt{D}, \qquad f_i = (f_{j,i})_{j=1}^{n}$$

define

$$F^r = (f_i^r)_{i=1,\ldots,m} = (f_{j,i}^r)_{\substack{j=1,\ldots,n \\ i=1,\ldots,m}}, \qquad f_{j,i}^r := \frac{f_{j,i}}{(\sum_k f_{j,k}^2)^{1/2}},$$

i.e. the $n \times m$ matrix F^r is calculate from the $n \times m$ matrix $(v_1 \sqrt{\lambda_1}, \ldots, v_m \sqrt{\lambda_m})$ by re-normalizing the n rows.

Let $U_1, \ldots, U_m$ denote independent Brownian motions, $U := (U_1, \ldots, U_m)^\top$. Then W defined by

$$\mathrm{d}W := (\mathrm{d}W_1, \ldots, \mathrm{d}W_n)^\top := F^r\, \mathrm{d}U$$

is an n-dimensional m-factorial Brownian motion.

2.1 Shape of the Factors (Principal Components)

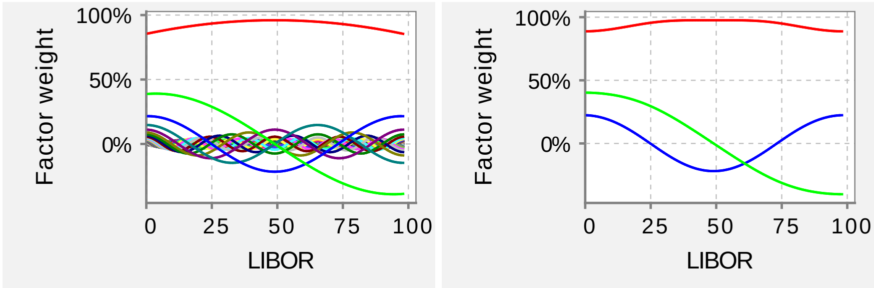

Figure 2.1. Factor reduction in the case of high correlation: The factors f_i (eigenvectors) of the correlation matrix $\rho_{i,j} = \exp(-0.005 * |i - j|)$ (left) and a reduction to the three factors having the largest eigenvalues (right).

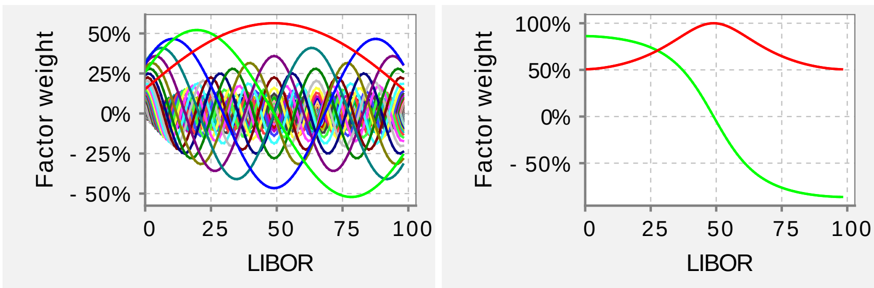

Figure 2.2. Factor reduction in the case of low correlation: The factors f_i (eigenvalues) of the correlation matrix $\rho_{i,j} = \exp(-0.1 * |i - j|)$ (left) and a reduction to the two factors having the largest eigenvalues (right).

2.2 Shape of the Correlation Matrix

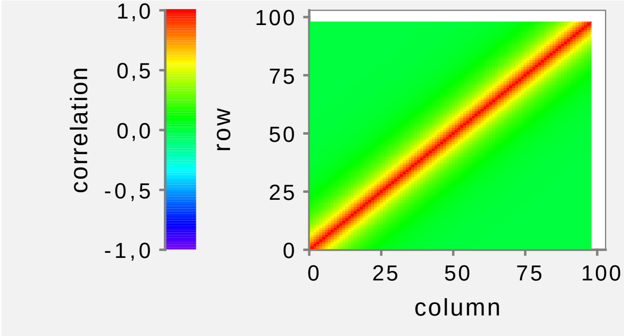

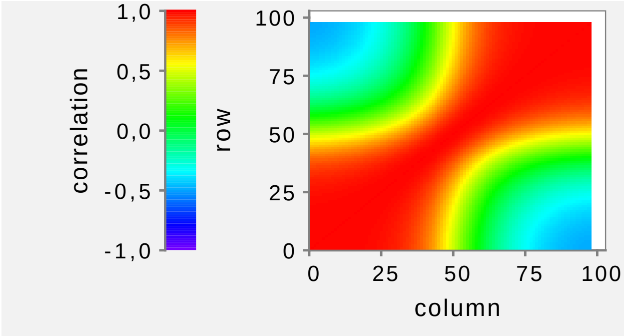

Figure 2.3. Factor reduction in the case of low correlation: The original correlation matrix $\rho_{i,j} = \exp(-0.1 * |T_i - T_j|)$ (top) and the correlation matrix corresponding to the reduction to two factors (bottom). This case corresponds to the factor reduction in Figure 2.2.

3 Shape of the Interest Rate Curve under Mean Reversion and a Multifactor Model

We consider a LIBOR market model with a simple covariance structure

$$\sigma_i(t) \;=\; \sigma^* \;\exp\left(-a\,(T_i - t)\right)$$

$$\rho_{i,j} \;=\; \exp(-r|T_i - T_j|).$$

We explore the interest rate curve $\{L_i(t) : i = 0, 1, 2, \ldots\}$ for different parameter configurations. We simulate under the terminal measure and start with an initially flat interest rate curve $L_i(0) = 0.1$, $i = 0, 1, 2, \ldots$. To summarize, our model framework consists of three degrees of freedom which will be varied in our analysis (see Table 3.1).

Parameter	Effect
a	Damping of the exponentially decaying, time-homogenous volatility
r	Damping of the exponentially decaying instantaneous correlation
m	Number of factors extracted from the correlation matrix

Table 3.1. Free parameters of the LIBOR market model considered.

3.1 Mean Reversion

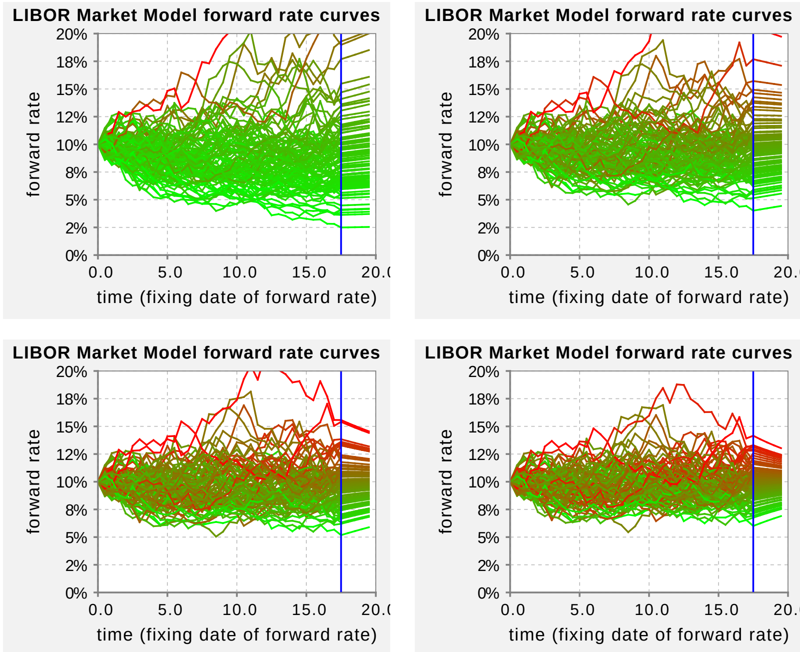

Figure 3.1. Shape of the fixed rates $L_i(T_i)$ and the interest rate curve for different instantaneous volatilities (corresponds to different mean reversion) frozen at time $t = 17.5$ using a one-factor mode. We used $a = 0$ (upper left), $a = 0.05$ (upper right), $a = 0.10$ (lower left) and $a = 0.15$ (lower right).

3.2 Factors

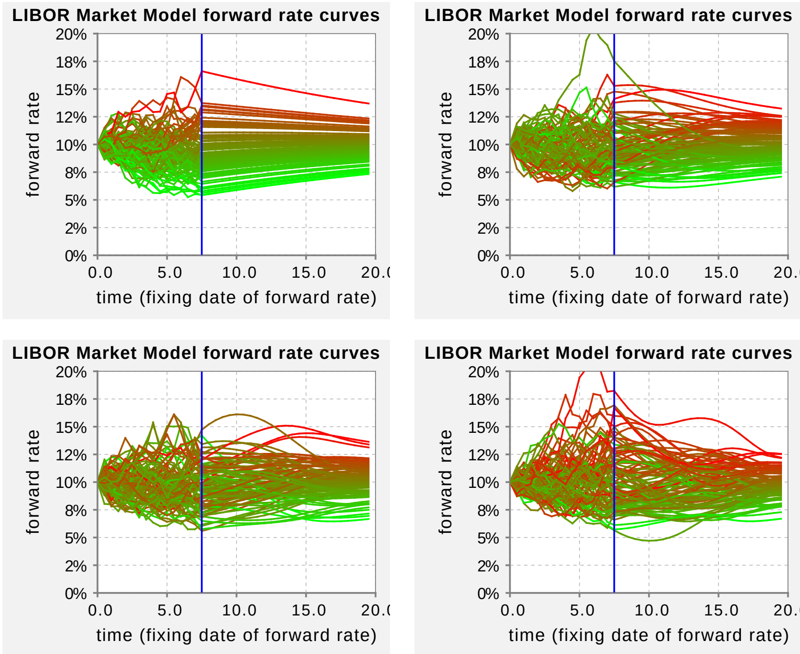

Figure 3.2. Shape of the interest rate curve with different factor configurations, seen at time $t = 7.5$: One, two, three, and five factors (from upper left to lower right).

3.3 Exponential Volatility Function

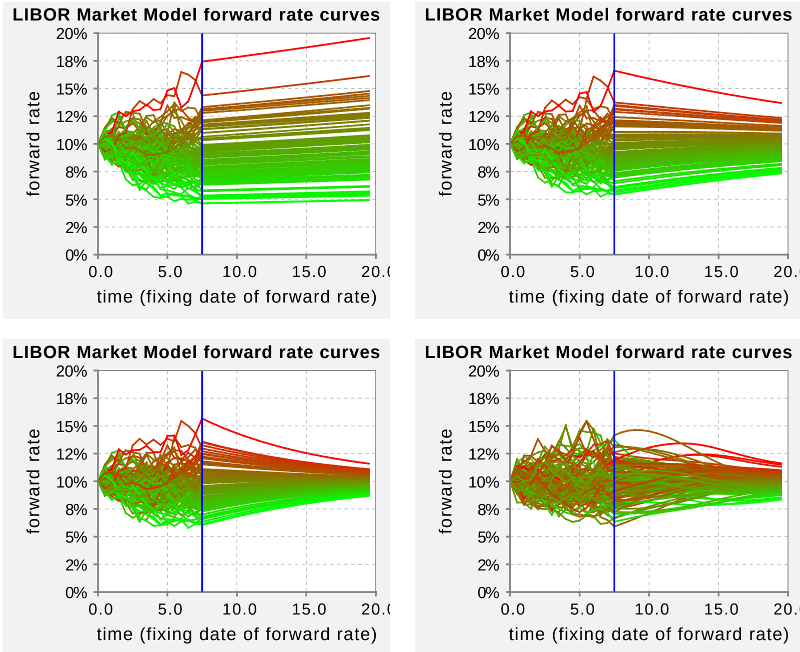

Figure 3.3. Shape of the fixed rates $L_i(T_i)$ and the interest rate curve with different instantaneous volatilities (corresponds to mean reversion) at time $t = 7.5$ in a one-factor model (upper row and lower left) with $a = 0.0$, $a = 0.05$ and $a = 0.1$ and a three-factor model (lower right) with $a = 0.1$.

3.4 Instantaneous Correlation

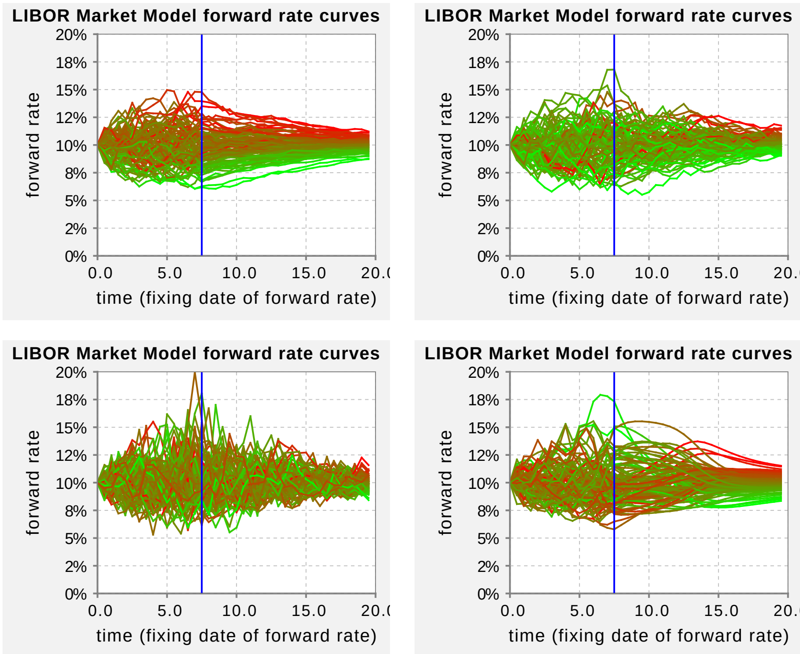

Figure 3.4. Shape of the fixed rates $L_i(T_i)$ and the interest rate curve with different instantaneous correlations, seen at time $t = 7.5$. We used a correlation matrix with (all) 40 factors and $r = 0.01$ (upper left, high correlation), $r = 0.1$ (upper right) and $r = 1.0$ (lower left, high de-correlation). In the lower right we used a correlation matrix with $r = 1.0$ (the same as in lower left), but reduced the number of factors to three.

4 Terminal Correlation and Terminal Distributions

In Section 4.1 we show how instantaneous volatility and correlation influence the terminal correlation of model quantities, here the LIBOR rates of a LIBOR market model. A terminal decorrelation may be achieved in a model with perfect instantaneous correlation (one factor model).

However, terminal distributions and terminal correlations depend on the chosen martingale measure. We depict this in Section 4.2.

4.1 Terminal Correlation Examined in a LIBOR Market Model Example

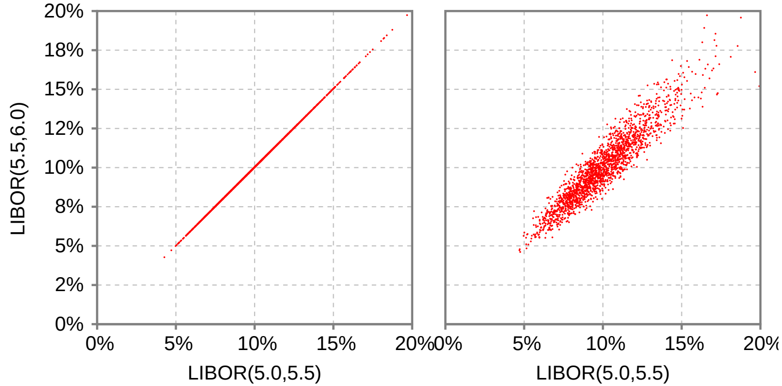

Figure 4.1. The two (adjacent) rates $L_{10} = L(5.0, 5.5)$ and $L_{11} = L(5.5, 6.0)$ in a one- and a multifactor model for constant instantaneous volatility $\sigma_{10}(t) = \sigma_{11}(t) = \text{const}$. In a one-factor model both random variables are perfectly correlated (left). In a five-factor model both random variables show a correlation different from 1. This is a consequence of the instantaneous correlation $\rho_{10,11}$ being different from 1.

Terminal Correlation Examined in a LIBOR Market Model Example

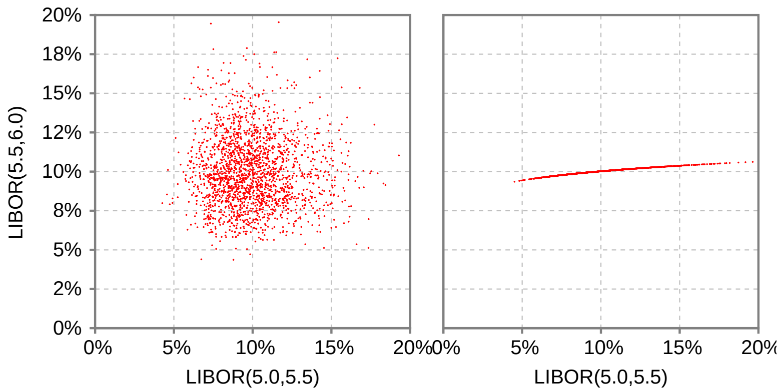

Figure 4.2. The two (adjacent) rates $L_{10} = L(5.0, 5.5)$ and $L_{11} = L(5.5, 6.0)$ in a one-factor model. Left: The two random variables exhibit a correlation close to 0 (perfect decorrelation). Right: The two random variables exhibit very different variances. The covariance is close to zero since the variance of L_{11} is close to 0. Both scenarios are the consequence of a very special choice for the instantaneous volatility.

4.2 Dependence of the Terminal Density on the Martingale Measure

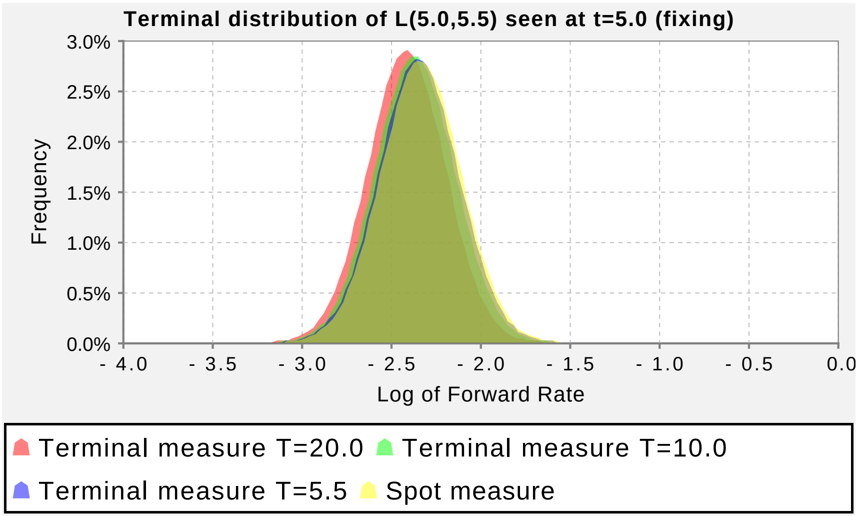

Figure 4.3. The terminal distribution function of a forward rate under different martingale measures. Shown is the rate $L(5.0, 5.5)$ upon its fixing at $t = 5.0$. All rates are simulated in a one-factor LIBOR market model with constant instantaneous volatility $\sigma = 10\%$.

Dependence of the Terminal Density on the Martingale Measure

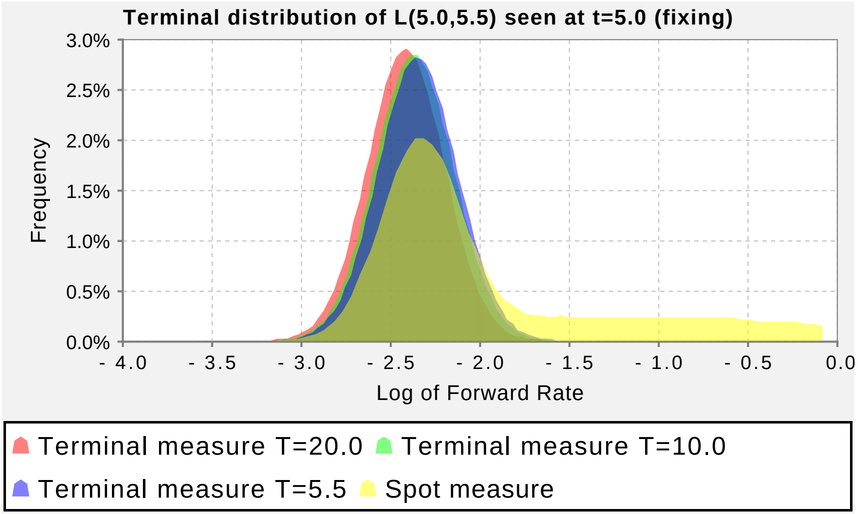

Figure 4.4. The terminal distribution function of a forward rate under different martingale measures. Shown is the rate $L(5.0, 5.5)$ upon its fixing at $t = 5.0$. In contrast to Figure 4.3 the rates $L(T_i, T_{i+1})$ for $T_i < 5.0$ are simulated differently. They are simulated with a high volatility of 150%. All other rates are simulated as in Figure 4.3 with volatility $\sigma = 10\%$. The change of the simulation of the other rates has an significant impact on the distribution of $L(5.0, 5.5)$ under the spot measure.

5 Proxy Simulation Schemes

5.1 Importance Sampling using a Proxy Scheme

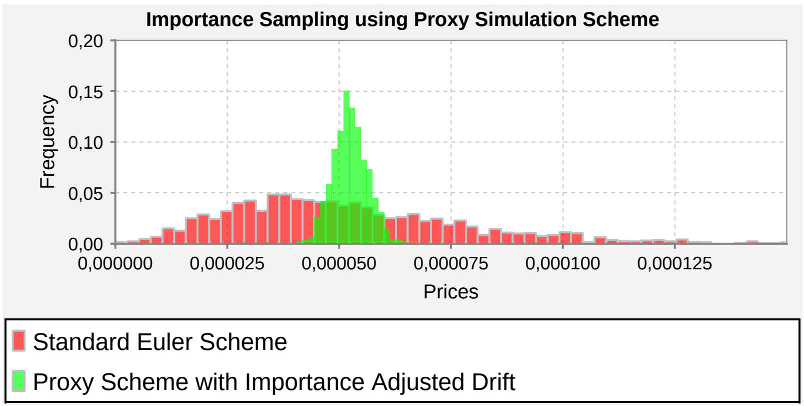

Figure 5.1. Importance sampling using a drift-adjusted proxy scheme. The example was created using a LIBOR market model to price a caplet with strike $K = 0.3$, the initial forward rate being $X_0 = L_i(0) = 0.1$.

5.2 Applying Finite Differences to a Full Proxy Scheme: Gamma of a TARN

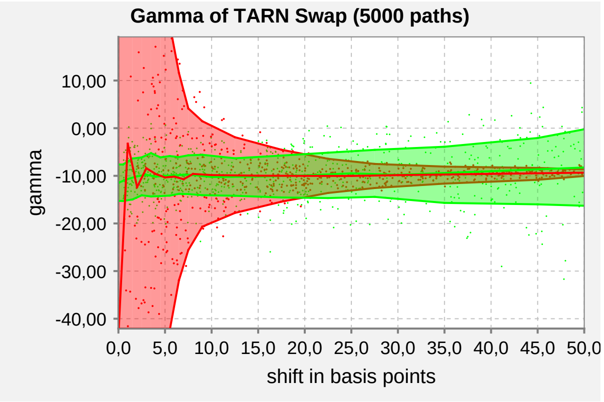

Figure 5.2. Dependence of the TARN gamma on the shift size of the finite difference approximation. Finite difference is applied to a direct simulation (red) and to a (partial) proxy scheme simulation (green). Each dot corresponds to one Monte-Carlo simulation with the stated number of paths. The red and green corridors represent the corresponding standard deviation.
The proxy scheme simulation shows no variance increase for small shift sizes while giving stable expected values for the sensitivity.

5.3 Applying Finite Differences to a Partial Proxy Scheme: Gamma of a TARN

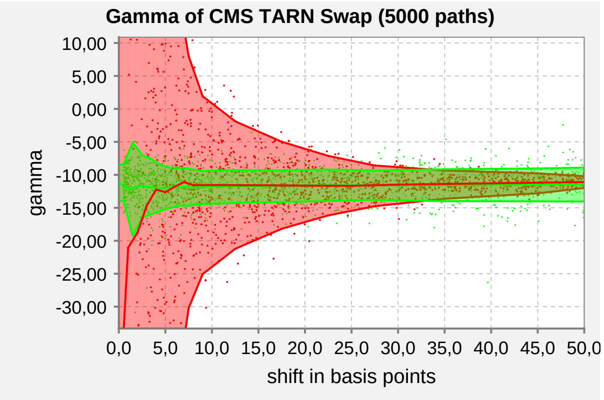

Figure 5.3. Dependence of the CMS TARN gamma on the shift size of the finite difference approximation. Finite difference is applied to a direct simulation (red) and to a (partial) proxy scheme simulation (green). The proxy constraint used was a simple (numerical) linearization of (**??**).

5.4 Applying Finite Differences to a Partial Proxy Scheme with Non-Linear Proxy Constraint: Gamma of a TARN

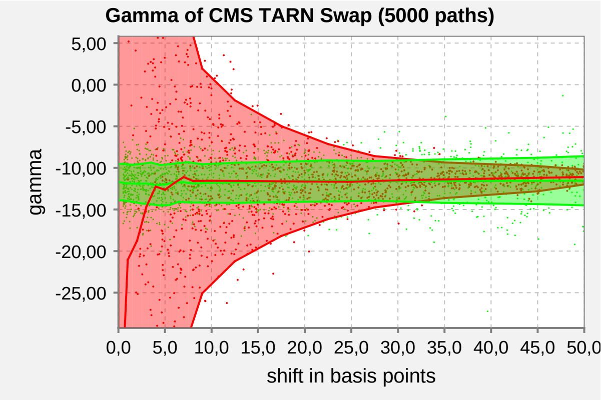

Figure 5.4. Dependence of the CMS TARN gamma on the shift size of the finite difference approximation. Finite difference is applied to a direct simulation (red) and to a (partial) proxy scheme simulation (green). The proxy constraint is given by applying a few Newton iterations to the (numerical) linearization of (**??**).

5.5 Applying Finite Differences to a Partial Proxy Scheme: Vega of a TARN

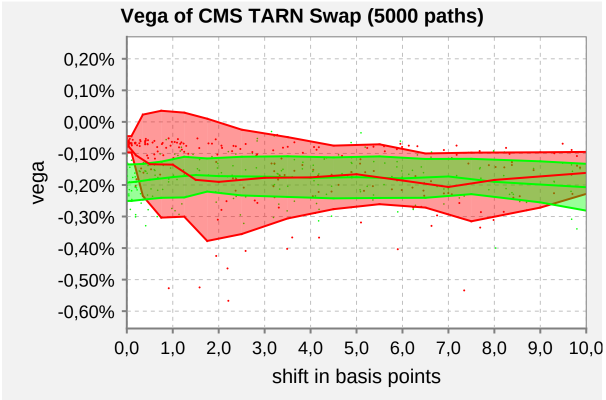

Figure 5.5. Dependence of the CMS TARN vega on the shift size of the finite difference approximation. Finite difference is applied to a direct simulation (red) and to a (partial) proxy scheme simulation (green). The proxy constraint was given by applying a few Newton iterations to the (numerical) linearization of (**??**).

5.6 Applying Finite Differences to a Direct Simulation: Delta of a Digital Caplet

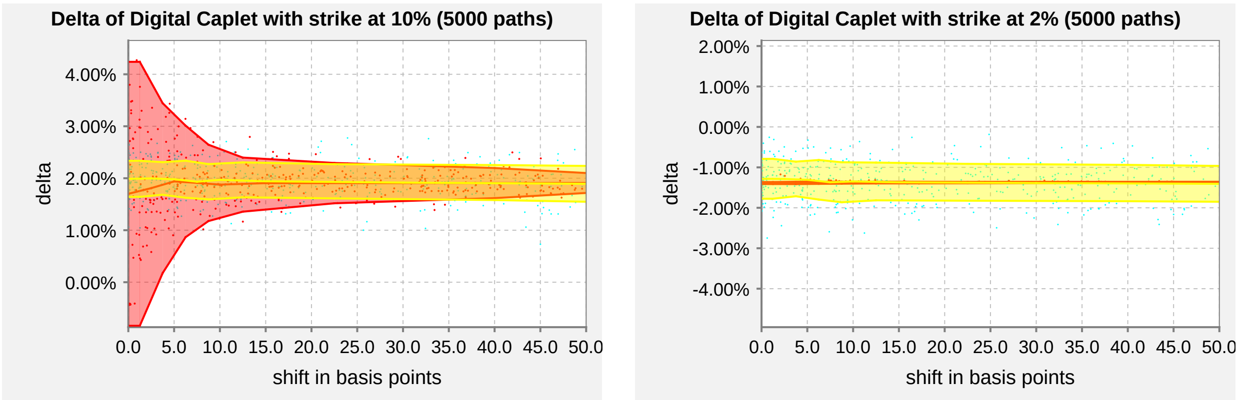

Figure 5.6. Delta of a digital caplet calculated by finite difference applied to direct simulation (red) and to a partial proxy scheme simulation, internally using the likelihood ratio method (yellow). The forward of the model is at $L(0) = 10\%$. If the the strike K is close to the forward (left figure, $K = L(0) = 10\%$) then the partial proxy scheme (likelihood ratio method) remains stable for small shifts, while the direct simulation (pathwise method) becomes unstable. If the strike K is far from the forward (right figure, $K = 2\%, L(0) = 10\%$) then the partial proxy scheme falls short of the direct simulation due to the huge Monte-Carlo variance introduced by the likelihood ratio.

5.7 Applying Finite Differences to Full and Partial Proxy Simulation Schemes: Gamma of a Digital Caplet

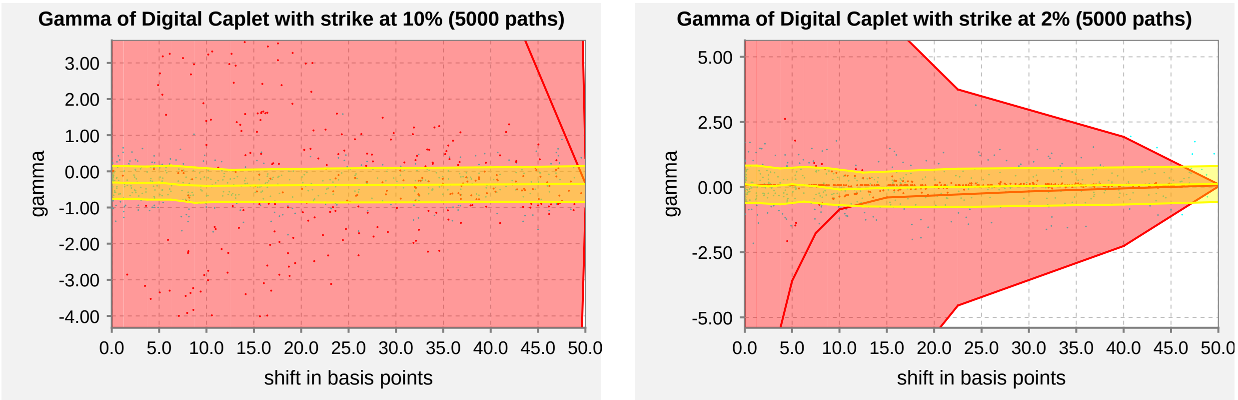

Figure 5.7. Gamma of a digital caplet calculated by finite difference applied to direct simulation (red) and to a partial proxy scheme simulation, internally using the likelihood ratio (yellow). For gamma the proxy simulation scheme is the method of choice in both cases, $K = L(0) = 10\%$ and $K = 2\%$.

5.8 Applying Finite Differences to a Localized Proxy Simulation Scheme: Delta

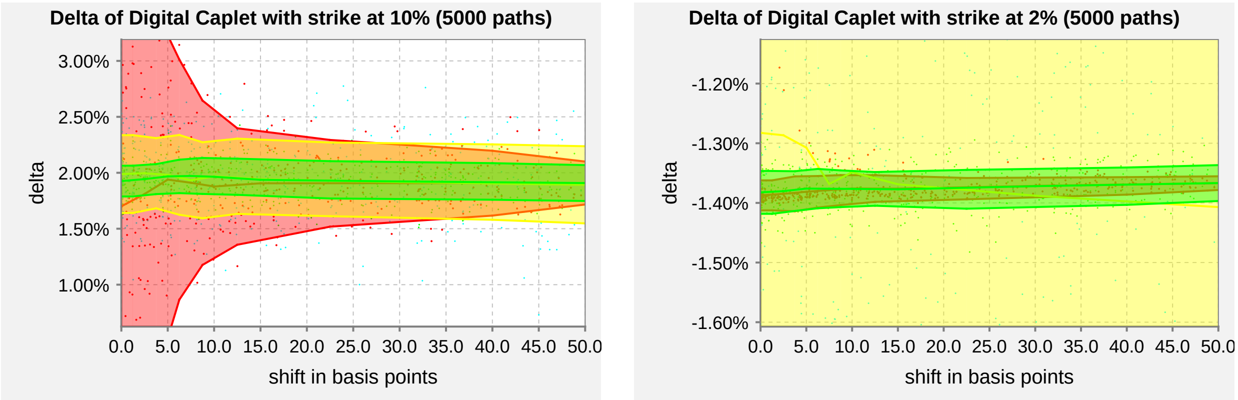

Figure 5.8. Delta of a digital caplet calculated by finite difference applied to direct simulation (red), to a partial proxy scheme simulation (yellow) and to a localized proxy simulation scheme (green). The initial forward rate of the model is at 10%. If the the strike K is close to the forward rate (left figure) then the partial proxy scheme (likelihood ratio method) remains stable for small shifts, while the direct simulation (pathwise method) becomes unstable. If the strike K is far away from the forward rate, the partial proxy scheme falls short of the direct simulation due to the huge Monte-Carlo variance introduced by the likelihood ratio.

5.9 Applying Finite Differences to a Localized Proxy Simulation Scheme: Gamma

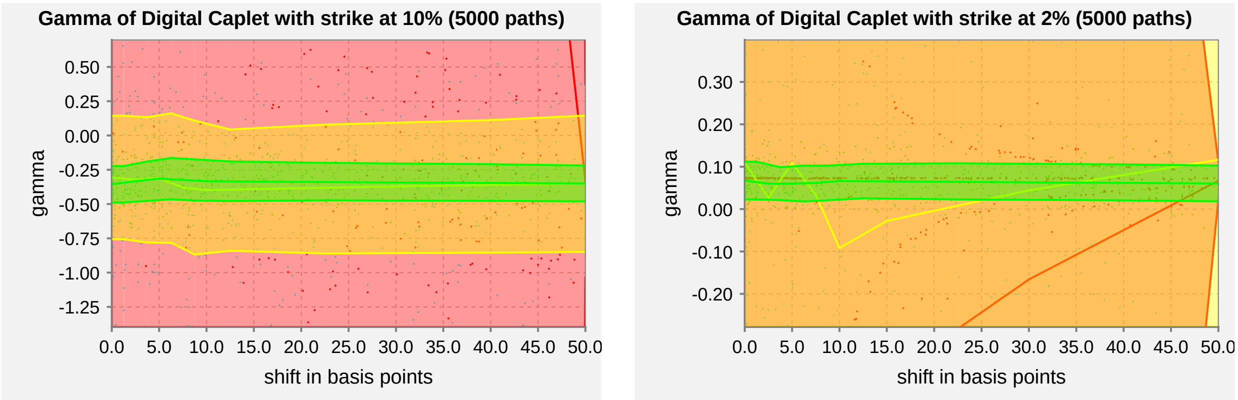

Figure 5.9. Gamma of a digital caplet calculate by finite difference applied to direct simulation (red), to a partial proxy scheme simulation (yellow) and to a localized proxy simulation scheme (green). As in Figure 5.6, considering different strikes shows that one or the other methods prevails.

5.10 Applying Finite Differences to a Localized Proxy Simulation Scheme: Delta of a TARN

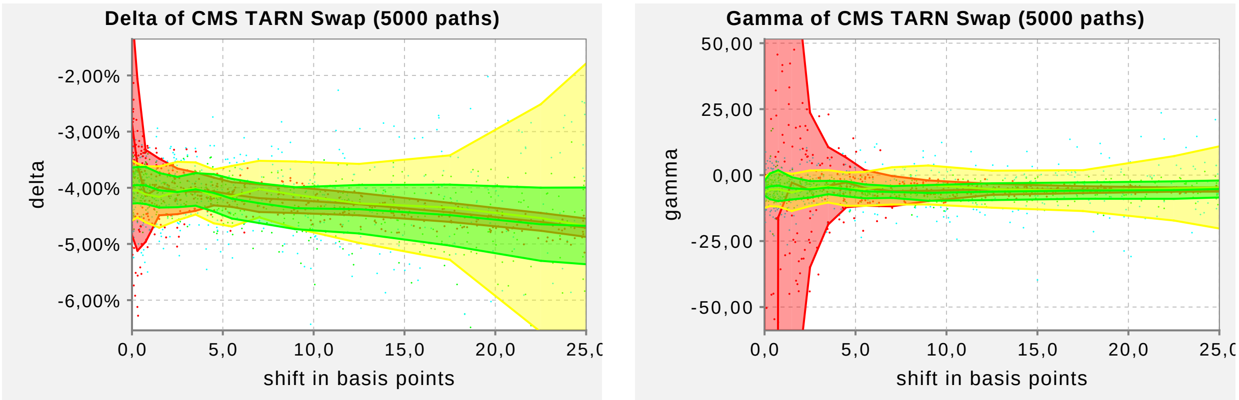

Figure 5.10. Delta and Gamma of a target redemption note (the coupon is a reverse CMS rate) calculated by finite difference applied to direct simulation (red), to a partial proxy scheme simulation (yellow) and to a localized proxy simulation scheme (green). Direct simulation produces enormous Monte-Carlo variances for small shift sizes. The method is useless. The partial proxy simulation scheme shows an increase in Monte-Carlo variance if the shift size is large. The localized proxy simulation scheme is an improvement on the partial proxy simulation scheme and shows only small Monte-Carlo variance for large shifts. Note: The localizer used is not the optimal one.

31 pages. 21 figures. 1 tables.